

Review Article

Nonlinear Optical Spectroscopy of Chiral Molecules

PEER FISCHER^{1*} AND FRANÇOIS HACHE²

¹*The Rowland Institute at Harvard, Harvard University, Cambridge, Massachusetts*

²*Laboratoire d'Optique et Biosciences, CNRS/INSERM/Ecole Polytechnique, Palaiseau, France*

ABSTRACT We review nonlinear optical processes that are specific to chiral molecules in solution and on surfaces. In contrast to conventional natural optical activity phenomena, which depend linearly on the electric field strength of the optical field, we discuss how optical processes that are nonlinear (quadratic, cubic, and quartic) functions of the electromagnetic field strength may probe optically active centers and chiral vibrations. We show that nonlinear techniques open entirely new ways of exploring chirality in chemical and biological systems: The cubic processes give rise to nonlinear circular dichroism and nonlinear optical rotation and make it possible to observe dynamic chiral processes at ultrafast time scales. The quadratic second-harmonic and sum-frequency-generation phenomena and the quartic processes may arise entirely in the electric-dipole approximation and do not require the use of circularly polarized light to detect chirality. They provide surface selectivity and their observables can be relatively much larger than in linear optical activity. These processes also give rise to the generation of light at a new color, and in liquids this frequency conversion only occurs if the solution is optically active. We survey recent chiral nonlinear optical experiments and give examples of their application to problems of biophysical interest.

© 2005 Wiley-Liss, Inc. *Chirality* 17:421–437, 2005.

KEY WORDS: review; nonlinear optics; spectroscopy; molecular chirality; optically active liquid; chiral monolayer; second-harmonic generation; SHG; sum-frequency generation; SFG; nonlinear circular dichroism; nonlinear optical activity; BioCARS

Natural optical activity comprises optical rotation (circular birefringence) and circular dichroism. Fresnel showed that a medium gives rise to optical rotation if its refractive indices for right- and left-circularly polarized light are unequal.¹ A difference in the corresponding absorption indices causes plane-polarized light to become elliptically polarized (circular dichroism). In optical activity phenomena, neither the angle of rotation of a polarized light beam nor its ellipticity is expected to change with the intensity of the light. However, at typical peak powers of pulsed lasers, the optical field strength can become comparable to the field that binds the valence electrons to the nucleus of an atom or a molecule, and under these conditions the optical properties will have contributions that depend nonlinearly on the applied electromagnetic fields. This is the realm of nonlinear optics.^{2–4} The usual linear refractive indices observed at low light intensities are then augmented by additional contributions that depend on the intensity of the light. Hence, nonlinear contributions to optical activity may be observed in optically active media under appropriate experimental conditions. We show that the cubic dependence on the electric field in nonlinear optical activity phenomena allows the observation of dynamic optical activity processes with unprecedented temporal resolution.

As we shall see, nonlinear optical phenomena may also give rise to the generation of light at a new wavelength. For instance, in sum-frequency generation, two laser beams that are in the visible may “mix” in a sample and generate light in the ultraviolet (UV). Surprisingly, such a process is only symmetry-allowed in a liquid, if the solution is optically active. In contrast to conventional optical activity, however, this nonlinear process can arise entirely from induced electric dipoles (without magnetic or quadrupolar transitions) and is not circular differential. Hence, no polarization modulation is needed, and the generated photons themselves are a measure of the solution's chirality. Because an achiral solvent cannot contribute to the signal, the technique is a sensitive, background-free probe of molecular chirality. In addition to the quadratic sum-frequency-generation process, which

Contract grant sponsor: Rowland Institute at Harvard

*Correspondence to: Dr. Peer Fischer, The Rowland Institute at Harvard, 100 Edwin H. Land Boulevard, Harvard University, Cambridge, MA 02142.
E-mail: fischer@rowland.harvard.edu

Received for publication 15 February 2005; Accepted 4 April 2005

DOI: 10.1002/chir.20179

Published online 4 August 2005 in Wiley InterScience
(www.interscience.wiley.com).

has been observed, a higher-order (quartic) nonlinear Raman spectroscopy (BioCARS) has been predicted to exist with similar properties. These techniques make it possible to access states of chiral molecules that lie in the UV as well as probe molecular vibrations with visible light. We discuss recent experiments and show how the application of an additional static electric field to sum-frequency generation allows the absolute configuration of the chiral solute to be determined.

Nonlinear spectroscopies can also be applied to oriented assemblies of (chiral) molecules. Such is the case with sum-frequency generation (SFG) and the bulk-forbidden but surface-specific second-harmonic generation process (SHG). Linear-polarized as well as circularly polarized light can probe the nonlinear optical response from a chiral molecular monolayer. Remarkably, the nonlinear intensity differentials in SHG can be much larger than for linear optical activity. For instance, the chiral SHG observable in a molecular film of a Tröger's base can be 6 orders of magnitude larger than the corresponding linear optical rotation. We give examples of SHG experiments on chiral surfaces of biological interest, including studies on proteins.

The aim of this review is to introduce the reader to the basic principles of chiral nonlinear optical spectroscopies and to give an overview of some recent experimental work. Although the use of chiral molecules as nonlinear optical materials is a major focus of current research, space does not permit us to discuss these in detail. The reader may consult the literature for further details.^{5–7}

We first outline some basic theoretical concepts that render certain nonlinear optical processes specific to chiral molecules.

THEORETICAL BACKGROUND

In this section, we consider the linear and nonlinear optical properties of molecules. We discuss the theoretical basis of linear^{2,8–11} and nonlinear optical activity as well as frequency conversion in chiral media.

Linear Optical Activity

Optical fields that are incident upon a molecule induce time-varying molecular moments which themselves radiate. Most linear optical phenomena such as refraction (and absorption) of light, and hence the refractive index (and the absorption index), as well as Rayleigh scattering can be interpreted through a molecule's oscillating electric-dipole moment $\vec{\mu}_{\text{ind}}$ linear in the electric field, \vec{E} ,^a

$$\vec{\mu}_{\text{ind}} = \vec{\alpha} \vec{E} + \dots, \quad (1)$$

where $\vec{\alpha}$ is the polarizability of the molecule. In general, $\vec{\alpha}$ relates the three components of the electric field vector to those of the dipole moment and is therefore a tensor with nine components. Molecular symmetry may reduce

the number of independent components. The induced dipole moments in an ensemble of molecules give rise to an average macroscopic polarization \vec{P} in the medium

$$\vec{P} = N \langle \vec{\mu}_{\text{ind}} \rangle, \quad (2)$$

where the angular brackets denote an orientational average over a region of space containing N molecules per unit volume. In analogy to eq. (1), we can write

$$\vec{P} = \epsilon_0 \vec{\chi}^{(1)} \vec{E} + \dots, \quad (3)$$

where ϵ_0 is the permittivity of the vacuum. The linear susceptibility $\vec{\chi}^{(1)}$ is the macroscopic analogue of the molecular polarizability. It relates the electric field vector to the macroscopic polarization vector. In a liquid, the linear susceptibility is a scalar and is related to the molecular polarizability via

$$\chi^{(1)} = \frac{N}{\epsilon_0} \frac{1}{3} (\alpha_{xx} + \alpha_{yy} + \alpha_{zz}) \equiv \frac{N}{\epsilon_0} \bar{\alpha}. \quad (4)$$

The linear refractive index n_0 of an isotropic, non-magnetic dielectric is a function of the susceptibility,

$$n_0 = (1 + \chi^{(1)})^{1/2} \equiv \sqrt{\epsilon}. \quad (5)$$

To describe the refractive index of an optically active liquid, it becomes necessary to go beyond the electric-dipole approximation in eq. (1), and to include the induced magnetic dipole moment \vec{m}_{ind} (and for oriented samples also the induced electric-quadrupole moment $\vec{\Theta}_{\text{ind}}$).¹² In analogy to eq. (2), the macroscopic magnetization and the macroscopic quadrupole density are respectively $\vec{M} = N \langle \vec{m}_{\text{ind}} \rangle$ and $\vec{Q} = N \langle \vec{\Theta}_{\text{ind}} \rangle$. For an optically active liquid, we need to consider^{8,13,14}

$$\begin{aligned} \vec{\mu}_{\text{ind}} &= \vec{\alpha} \vec{E} + \omega^{-1} \vec{G}' \dot{\vec{B}} + \dots, \\ \vec{m}_{\text{ind}} &= -\omega^{-1} \vec{G}' \dot{\vec{E}} + \dots, \end{aligned} \quad (6)$$

where the dot denotes a derivative with respect to time, and where \vec{G}' is the optical rotation tensor,^b which is a function of the rotational strength.

We now consider a monochromatic circularly polarized plane wave traveling along the z direction. In an optically active medium, the electric field \vec{E}^{\pm} with amplitude E_0 , and the magnetic field \vec{B}^{\pm} can (at a point $z = 0$) be written as

$$\begin{aligned} \vec{E}^{\pm} &= E_0 (\vec{x} \cos(\omega t) \mp \vec{y} \sin(\omega t)), \\ \vec{B}^{\pm} &= E_0 \frac{n_0}{c} (\pm \vec{x} \sin(\omega t) + \vec{y} \cos(\omega t)). \end{aligned} \quad (7)$$

The upper sign corresponds to right circularly polarized and the lower sign to left circularly polarized light; \vec{x}

^aIn condensed media, such as liquids, the field at the molecule will be different from the applied optical electric field, \vec{E} , due to induced dipole-dipole interactions of the surrounding molecules. \vec{E} in microscopic expressions, such as eq. (1), should be replaced with a "local field," which is approximated in the Lorentz model by $((\epsilon + 2)/3)\vec{E}$.

^bNote that some authors use $\vec{\beta}$ for the optical rotation tensor. However, in this article $\vec{\beta}$ is used to describe a nonlinear optical property tensor, the first hyperpolarizability.

and \vec{y} are unit vectors; and c is the speed of light in a vacuum.

Substitution of the fields into $\vec{\mu}_{\text{ind}}$ in eq. (6) and use of eq. (3) yield

$$\vec{P}^{\pm} = \varepsilon_0 \left(\frac{N\bar{\alpha}}{\varepsilon_0} \pm \frac{N\bar{G}'n_0}{\varepsilon_0 c} \right) \vec{E}^{\pm} \quad (8)$$

for a liquid, where the isotropic component $\bar{G}' \equiv (G'_{xx} + G'_{yy} + G'_{zz})/3$. The induced magnetic dipole term is best included by considering an effective polarization that contains the contributions due to the magnetization and the quadrupole density^{15,16}

$$\vec{P}_{\text{eff}} = \vec{P} + \frac{i}{\omega} \vec{\nabla} \times \vec{M} - \vec{\nabla} \cdot \vec{Q}, \quad (9)$$

such that

$$\vec{P}_{\text{eff}}^{\pm} = \varepsilon_0 \left(\frac{N\bar{\alpha}}{\varepsilon_0} \pm \frac{2N\bar{G}'n_0}{\varepsilon_0 c} \right) \vec{E}^{\pm} \quad (10)$$

The effective polarization is of the form

$$\vec{P}_{\text{eff}} = \varepsilon_0 \chi_{\text{eff}} \vec{E}, \quad (11)$$

and since the refractive index of a dielectric is, in general, given by $n = (1 + \chi_{\text{eff}})^{1/2}$, we obtain the refractive index of an optically active liquid for right (+) and left (−) circularly polarized light:

$$n^{(\pm)} \approx n_0 \pm g_0, \quad \text{where } g_0 = \frac{N\bar{G}'}{\varepsilon_0 c}. \quad (12)$$

The optical rotation in radians developed over a path length l is a function of the wavelength λ and the circular birefringence and is given by:⁸

$$\vartheta = \frac{\pi l}{\lambda} (n^{(-)} - n^{(+)}). \quad (13)$$

We thus obtain the familiar Rosenfeld equation for optical rotation:

$$\vartheta \approx -\frac{2\pi l}{\lambda} g_0. \quad (14)$$

Nonlinear Optical Activity

In order to describe nonlinear optical contributions to the refractive index we need to consider the induced moments expanded in powers of the electromagnetic field. The induced electric-dipole moment of eq. (1) oscillating at ω becomes

$$\vec{\mu}_{\text{ind}} = \vec{\alpha} \vec{E} + \vec{\gamma} \vec{E} \vec{E} \vec{E} + \dots \quad (15)$$

For an electric field $\vec{E} \propto \vec{E}_0 \cos(\omega t)$, the term that is cubic in the electric field has a time dependence $\cos^3(\omega t)$.

Because $\cos^3(\omega t) \propto 3 \cos(\omega t) + \cos(3\omega t)$, there is a term that varies as $\cos(\omega t)$ and therefore contributes to the refractive index at ω . The term that is quadratic in the electric field $\vec{\beta} \vec{E} \vec{E}$ has been omitted from eq. (15) as it has no term that oscillates at the input angular frequency ω . $\vec{\beta}$ and $\vec{\gamma}$ are known as the first and second hyperpolarizabilities, respectively. The first hyperpolarizability $\vec{\beta}$ gives rise to second-harmonic generation and sum-frequency generation (vide infra). It is seen that several nonlinear optical processes may occur simultaneously and that the respective hyperpolarizabilities are distinguished by their frequency argument.

The refractive index that includes the nonlinear (intensity-dependent) electric-dipolar contribution immediately follows from eqs. (2) and (15). We define $\chi^{(3)} \equiv N\vec{\gamma}/\varepsilon_0$ and write

$$\vec{P} = \varepsilon_0 \left(\chi^{(1)} + \chi^{(3)} |\vec{E}_0|^2 \right) \vec{E}, \quad (16)$$

such that (cf. eq. (11)) $n \approx n_0 + \chi^{(3)} |\vec{E}_0|^2 / (2n_0)$.^c We can write the refractive index in terms of the intensity, $I \propto |\vec{E}_0|^2$, and use a more compact notation by introducing the nonlinear index of refraction, n_2 :⁴

$$n \approx n_0 + n_2 I. \quad (17)$$

By considering the cubic field terms in eq. (6), the intensity-dependent refractive index of an optically active liquid can be derived in a similar fashion. Inspection of eqs. (12) and (17) suggests its general form:

$$n^{(\pm)} \approx (n_0 + n_2 I) \pm (g_0 + g_2 I), \quad (18)$$

where we have introduced a “nonlinear optical activity index,” g_2 . Hence, the circular birefringence of an optically active liquid is modified in the presence of intense light. In analogy to the Rosenfeld equation, we can write a generalized equation that describes linear and nonlinear optical rotation:

$$\vartheta \approx -\frac{2\pi l}{\lambda} (g_0 + g_2 I). \quad (19)$$

The corresponding absorption indices describe linear and nonlinear circular dichroism.

Nonlinear optical phenomena may not only modify the refractive index of an optically active liquid, but they can also generate light at wavelengths different from those of the incident laser. We now discuss such frequency-conversion processes that are specific to chiral molecules in liquids and on surfaces.

^cOther definitions of the fields and polarizations can be found in the nonlinear optics literature. The numerical factors that enter the expression for the refractive index and that accompany the susceptibilities (here and elsewhere in this paper) may therefore differ from those used in other conventions.

Coherent Frequency Conversion Processes in Chiral Media

The induced dipole quadratic in the electric field,

$$\vec{\mu}_{\text{ind}} = \vec{\beta} \vec{E} \vec{E}, \quad (20)$$

with $\vec{E} \propto \vec{E}_0 \cos(\omega t)$, has a static term and a term that oscillates at twice the applied frequency, since $\cos^2(\omega t) \propto 1 + \cos(2\omega t)$. The induced dipole oscillating at 2ω radiates and is the source of second-harmonic generation. Should the incident optical field contain two frequencies ω_1 and ω_2 , then radiation at the sum-frequency ($\omega_1 + \omega_2$) and the difference-frequency ($\omega_1 - \omega_2$) may be generated. Only sum (and difference) frequencies can be generated in a liquid, and only if the liquid is optically active.

Sum-frequency generation in liquids. The polarization for a sum-frequency-generation process is in general described by^d

$$\vec{P}(\omega_1 + \omega_2) = \varepsilon_0 \vec{\chi}^{(2)}(\omega_1 + \omega_2) \vec{E}(\omega_1) \vec{E}(\omega_2), \quad (21)$$

where the second-order susceptibility tensor $\vec{\chi}^{(2)}$ is written with its frequency argument.

The intensity of the sum frequency is proportional to $|\vec{P}(\omega_1 + \omega_2)|^2$. In a liquid, one needs to consider an isotropic average in eq. (21) with the result that the polarization is given by the vector cross product of the incident fields

$$\vec{P}(\omega_1 + \omega_2) = \varepsilon_0 \chi^{(2)}(\omega_1 + \omega_2) (\vec{E}(\omega_1) \times \vec{E}(\omega_2)), \quad (22)$$

and the susceptibility (for one enantiomer) is a scalar of the form

$$\begin{aligned} \chi^{(2)} &= \frac{N}{\varepsilon_0} \frac{1}{6} (\beta_{xyz} - \beta_{xzy} + \beta_{yzx} - \beta_{yxz} + \beta_{zyx} - \beta_{zxy}) \\ &\equiv \frac{N}{\varepsilon_0} \bar{\beta}. \end{aligned} \quad (23)$$

The term in parentheses vanishes for any molecule that possesses reflection planes, a center of inversion, or rotation-reflection axes, and $\bar{\beta}$ is thus only nonzero for a chiral molecule.^e It is of opposite sign for the enantiomers of a chiral molecule. $\bar{\beta}$ is therefore a pseudoscalar (a scalar that changes sign under parity), as are the chirality

observables \bar{G} , g_0 , and g_2 . However, in contrast to linear and nonlinear optical activity phenomena, $\bar{\beta}$ arises entirely in the electric-dipole approximation (no magnetic or electric-quadrupolar contributions). $\chi^{(2)}$ is zero in a racemic mixture, as here the number densities for the R- and S-enantiomers are equal and their contributions to eq. (23) cancel. Sum-frequency generation in a liquid is thus in itself a measure of a solution's chirality.

Second-harmonic and sum-frequency generation at surfaces. Second-harmonic generation cannot occur in a liquid, even if the solution is optically active.^f In SHG $\omega_1 = \omega_2$ and the hyperpolarizability components in eq. (23) become symmetric in the corresponding indices, e.g., $\beta_{xyz} = \beta_{xzy}$ etc., such that their antisymmetric sum vanishes. However, both sum-frequency generation (SFG) and second-harmonic generation (SHG) are allowed at a surface provided the molecules at the interface adopt a preferred orientation. This is, for instance, the case for a thin layer of dipolar molecules that lie between two isotropic media with different optical properties, such as the liquid/air interface. Generally, one assumes that such a surface is symmetric about its normal, giving C_∞ symmetry for chiral molecules and $C_{\infty v}$ for achiral molecules. The interface is then characterized by one axis, the surface normal, around which it is rotationally invariant and which is parallel to the direction of the average dipole moment. In addition, the arrangement of the molecules at the interface can often be characterized by an average tilt angle θ of the molecular axis (taken to be along "z") with respect to the surface normal (along "Z"). The nonvanishing components of the second-order surface susceptibility tensor, evaluated in the frame of the laboratory that contains the optical fields, are then related to the first hyperpolarizability tensor, which is expressed in molecular coordinates, by the following matrix equations:^{17,18}

$$\begin{pmatrix} \chi_{ZZZ}^{(2)} \\ \chi_{ZXX}^{(2)} \\ \chi_{XZZ}^{(2)} \\ \chi_{XXZ}^{(2)} \end{pmatrix} = \frac{N_\sigma}{\varepsilon_0} \begin{bmatrix} a & 2b & 2b & 2b \\ 2b & c & -b & -b \\ 2b & -b & c & -b \\ 2b & -b & -b & c \end{bmatrix} \times \begin{pmatrix} \beta_{zzz} \\ \beta_{zxx} + \beta_{zyy} \\ \beta_{xzx} + \beta_{yzy} \\ \beta_{xxz} + \beta_{yyz} \end{pmatrix}, \quad (24)$$

where N_σ is the number of molecules per unit area and where $a = \cos^3\theta$, $b = \frac{1}{4}(\cos\theta - \cos^3\theta)$, $c = \frac{1}{4}(\cos\theta + \cos^3\theta)$. In addition, the following identities hold:

$$\chi_{ZXX}^{(2)} = \chi_{ZYX}^{(2)}, \chi_{XZZ}^{(2)} = \chi_{YZX}^{(2)}, \chi_{XXZ}^{(2)} = \chi_{YYZ}^{(2)}.$$

^dThe polarization oscillating at the sum frequency is the source of a new wave, so that one has to consider the interaction of several (incident and generated) coupled waves in the medium. Efficient frequency conversion occurs when the vector sum of the incoming photon momenta matches the momentum of the generated wave (phase-matching).

^eParity, or space inversion, is the symmetry operation that interconverts the enantiomers of a chiral molecule. Under space inversion all coordinates (x, y, z) are replaced everywhere by $(-x, -y, -z)$.⁸ It follows that under parity all the hyperpolarizability tensor components in eq. (23) change sign, e.g., $\beta_{xyz} \xrightarrow{\text{Parity}} \beta_{(-x)(-y)(-z)} = -\beta_{xyz}$. Hence, the antisymmetric sum ($\bar{\beta}$) in eq. (23) also changes sign under parity.

^fNo coherent SHG, whether electric-dipolar or magnetic-dipolar/electric-quadrupolar, can be generated in the bulk of a liquid if the incident fields are plane waves. Only near a surface can multipolar "bulk" SHG give rise to a traveling wave.

For chiral molecules, there are additional components

$$\begin{pmatrix} \chi_{XYZ}^{(2)} \\ \chi_{YZX}^{(2)} \\ \chi_{ZXY}^{(2)} \end{pmatrix} = \frac{N_\sigma}{\varepsilon_0} \begin{bmatrix} d & e & e \\ e & d & e \\ e & e & d \end{bmatrix} \begin{pmatrix} \beta_{xyz} - \beta_{yxz} \\ \beta_{yzx} - \beta_{xzy} \\ \beta_{zxy} - \beta_{zyx} \end{pmatrix}, \quad (25)$$

where $d = \frac{1}{2}\cos^2\theta$, $e = \frac{1}{4}(1 - \cos^2\theta)$, and where

$$\chi_{XYZ}^{(2)} = -\chi_{YXZ}^{(2)}, \chi_{YZX}^{(2)} = -\chi_{XZY}^{(2)}, \chi_{ZXY}^{(2)} = -\chi_{ZYX}^{(2)}.$$

The matrix equations above hold for SFG and SHG. In addition, the following identities apply in the case of SHG:

$$\begin{aligned} \chi_{XZX}^{(2)} &= \chi_{XXZ}^{(2)} = \chi_{YZY}^{(2)} = \chi_{YYZ}^{(2)}, \\ \chi_{XYZ}^{(2)} &= -\chi_{YXZ}^{(2)} = -\chi_{YZX}^{(2)} = \chi_{XZY}^{(2)}. \end{aligned} \quad (26)$$

Only chiral molecules, i.e., molecules with the point-group symmetry C_n , D_n , O , T , or I , can give rise to the surface susceptibility elements in eq. (25). Hence an experimental geometry that probes one of the “XYZ” surface-susceptibility elements is a probe of molecular chirality. For example, any Y-polarized SHG that is observed in reflection from a C_∞ surface, when the input beam is polarized parallel to the plane of incidence (ZX), requires the surface to be chiral. The components of the polarization from the surface are in this case given by

$$P_Y(2\omega) = 2\varepsilon_0\chi_{YXZ}^{(2)} \cos \varphi \sin \varphi |\vec{E}_0(\omega)|^2, \quad (27)$$

where φ is the angle of incidence. In addition, there will be achiral contributions

$$\begin{aligned} P_Z(2\omega) &= \varepsilon_0 \left(\chi_{ZZZ}^{(2)} \sin^2 \varphi + \chi_{ZXX}^{(2)} \cos^2 \varphi \right) |\vec{E}_0(\omega)|^2, \\ P_X(2\omega) &= 2\varepsilon_0\chi_{XZZ}^{(2)} \cos \varphi \sin \varphi |\vec{E}_0(\omega)|^2, \end{aligned} \quad (28)$$

where we have used the identities in eq. (26). The second-harmonic’s plane of polarization is thus seen to “rotate” as a function of $\chi_{YXZ}^{(2)}$ and as a function of the enantiomeric excess at the interface. This effect has been termed “SHG-ORD.”¹⁹ Similarly, the circular SHG intensity differential has been termed “SHG-CD,” and “SHG-LD” describes linear SHG intensity differentials.²⁰ These descriptions are widely used, and we follow this practice in this review. However, we would like to stress that these SHG processes do not arise from differences in the refractive and absorption indices that respectively underlie optical rotatory dispersion and circular dichroism in linear optical activity.

This completes our theoretical overview, and we now turn to the application of these concepts.

SUM-FREQUENCY GENERATION IN CHIRAL LIQUIDS

In sum-frequency-generation (SFG) spectroscopy, the pulses from a laser are overlapped in a medium and the light generated at the sum of the two incident frequencies is detected. The light at the sum-frequency is a co-

herent and highly directional beam, and SFG is routinely used in crystals to generate radiation at wavelengths different from those of the available laser. As discussed in the preceding section, electric-dipolar SFG cannot occur in a medium that has a center of symmetry. SFG is therefore excluded in liquids, unless they are optically active: The intrinsic symmetry-breaking in chiral molecules causes a nonracemic liquid to be non-centrosymmetric and, as predicted by Giordmaine, allows for electric-dipolar SFG.²¹ Sum-frequency generation from chiral liquids has recently been reexamined²² and has been observed experimentally.^{23–28} We now discuss some of its salient features.

The induced electric-dipole polarization radiating at the sum-frequency is in a liquid given by eq. (22),

$$\vec{P}(\omega_1 + \omega_2) = \varepsilon_0\chi^{(2)}(\omega_1 + \omega_2) \left(\vec{E}(\omega_1) \times \vec{E}(\omega_2) \right),$$

where $\vec{E}(\omega_1)$ and $\vec{E}(\omega_2)$ are monochromatic fields that oscillate with frequency components ω_1 and ω_2 , respectively. It follows from the vector cross product that the electric fields at ω_1 , ω_2 , and $(\omega_1 + \omega_2)$ need to span the X, Y, and Z directions of a Cartesian frame. This requires a non-collinear beam geometry with one s-polarized and two p-polarized beams.²⁹ Whereas linear optical activity probes chirality with left- and right-circularly polarized light, the chiral probe in SFG corresponds to the three field directions which either form a left-handed or a right-handed coordinate frame. Chiral SFG spectroscopy therefore needs no circularly polarized light and no polarization modulation. Rather, it is the detection of photons at the sum frequency that constitutes the chiral measurement.

One can immediately see that there can be no chiral probe if two of the three waves have the same frequency, as is the case for SHG. The electric field vectors of the two frequency-degenerate fields add, and the three waves no longer make a coordinate frame. This is also borne out by the quantum mechanical expression for $\vec{\beta}$ which is proportional to $\omega_1 - \omega_2$ and therefore goes to zero for SHG, where $\omega_1 = \omega_2$.³⁰

As discussed in the introductory material, $\chi^{(2)}$ is the rotationally averaged component of the second-order susceptibility and is a pseudoscalar. For a solution that contains only two optically active molecular species, namely, the R- and S-enantiomers of a chiral molecule, we can write the isotropic part of the electric-dipolar second-order susceptibility as

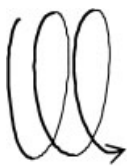
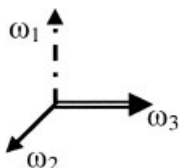
$$\chi^{(2)} = \frac{1000N_A}{\varepsilon_0} ([R] - [S])\vec{\beta}_R, \quad (29)$$

where the square brackets denote a concentration in mol/l, and where N_A is Avogadro’s number. $\vec{\beta}_R$ is the $\vec{\beta}$ of the R-enantiomer and is given by

$$\begin{aligned} \vec{\beta}_R &= \frac{1}{6} (\beta_{R,xyz} - \beta_{R,xzy} + \beta_{R,yzx} - \beta_{R,yxz} + \beta_{R,zyx} \\ &\quad - \beta_{R,zyx}), \end{aligned} \quad (30)$$

as is required for a pseudoscalar, $\bar{\beta}_R = -\bar{\beta}_S$, so that $\chi^{(2)}$ is zero for a racemic solution (where $[R] = [S]$). The intensity at the sum frequency is proportional to $|\chi^{(2)}|^2$, and the sum-frequency signal thus depends quadratically on the difference in concentration of the two enantiomers. A sum-frequency experiment therefore measures the chirality of a solution and not its handedness, and SFG does not distinguish between optical isomers.³¹ This is shown in Figure 1, where a quadratic dependence of a SFG signal on the (fractional) concentration difference of the R-(+) and S-(−) enantiomers of 1,1'-bi-2-naphthol (BN) is observed.²⁵ Within the noise of the experiment, no signal is recorded for the racemic mixture. SFG is thus effectively background free: any achiral signals (solvent, higher-order multipolar contributions) are either too weak to be observed or can be eliminated by choosing appropriate beam polarizations. As seen in Table 1, this is in contrast to linear optical activity phenomena, which always contain an achiral and a chiral response. Several other differences between optical activity and chiral SFG are also listed in Table 1. For instance, linear optical activity phenomena require both electric-dipolar as well as magnetic-dipolar transitions, whereas SFG from an optically active liquid is entirely electric-dipolar. This is significant, as magnetic-dipole (and electric-quadrupole) transitions are typically much weaker than electric-dipole transitions. Nevertheless, the absolute strength of the SFG signals is low. In principle, this is not a problem, as it is possible to detect low light levels with single-photon counting methods, especially as there is little or no background in SFG. However, in practice at least one of the three frequencies needs to be near or on (electronic or vibrational) resonance for there to be a measurable SFG signal. The concomitant linear absorption further limits the conversion efficiency, which is already low as the SFG process cannot be phase-matched in liquids.

TABLE 1. Comparison between linear optical activity and nonlinear optical sum-frequency generation as probes of molecular chirality in liquids

	Optical activity	Nonlinear optics (SFG)
pseudoscalar	$\bar{G}' \propto \omega \text{Im}[\vec{\mu}_{gm} \cdot \vec{m}_{mg}]$ electric- and magnetic-dipolar	$\bar{\beta} \propto (\omega_1 - \omega_2) \vec{\mu}_{gm} \cdot$ $[\vec{\mu}_{mn} \times \vec{\mu}_{ng}]$ electric-dipolar
signal	chiral and achiral response	only chiral response, no background
experiment: chiral probe	 cp light	 linearly polarized beams
observable	different response to cp light $\sim \bar{G}'$	intensity at sum frequency $\sim \bar{\beta} ^2$

Ab initio calculations and $\bar{\beta}$ of binaphthol. Quantum chemical calculations on several chiral molecules confirm that the SFG pseudoscalar $\bar{\beta}$ is, even near resonance, much weaker than a regular nonzero tensor component of the first hyperpolarizability.^{22,26,32–34} Since $\bar{\beta}$ has no static limit, its dispersion is, however, much more dramatic. Figure 2 shows the enhancement by many orders of magnitude that the SFG signal (which is proportional to the square of $\bar{\beta}$) from BN experiences over a relatively small wavelength range.²⁶ The mechanism of the nonlinear response in BN has been computed ab initio,^{26,35,36}

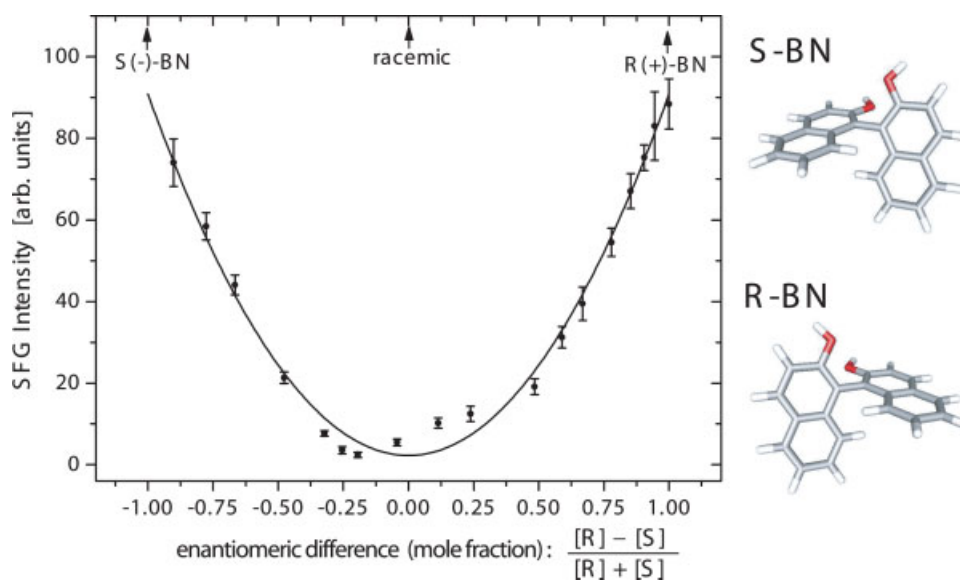


Fig. 1. Structures of 1,1'-bi-2-naphthol (BN) and continuous titration of two 0.5 M solutions of R-(+)-BN and S-(−)-BN in tetrahydrofuran. The sum-frequency intensity is observed at 266 nm with the incident beams at 800 and 400 nm. (Adapted from ref. 25).

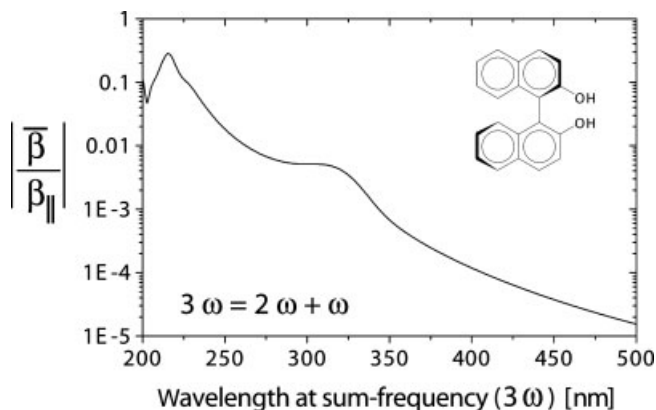


Fig. 2. The dispersion of the chirality specific pseudoscalar $\tilde{\beta}$ is shown relative to that of the (achiral) vector component of the first hyperpolarizability β_{\parallel} for the sum-frequency generation process $3\omega = 2\omega + \omega$ in optically active 1,1'-bi-2-naphthol (configuration action singles sum-over-states computation; Hartree-Fock theory with a cc-pVDZ basis set). (Adapted from ref. 26).

and its (vibronic) exciton chirality^{26,35} has been discussed in terms of coupled-oscillator models.^{35,37–39,109} The nonlinearity of BN is predominantly electric-dipolar³⁵ (see also the section “*Molecular origin of chiral SHG*”). Recent experiments show that nonlocal higher-order multipolar (magnetic and electric quadrupolar) contributions to SFG from BN are measurable and that they are indeed much weaker than the electric-dipolar nonlinearity.²⁶ We stress that selecting the polarization of all three fields in bulk SFG allows the chiral electric-dipolar signals to be discerned from any achiral (magnetic-dipolar and electric-quadrupolar) SFG signals. In two recent ab initio studies on helical π -conjugated molecules, such as helicenes and heliphenes, Champagne and co-workers predict that the nonresonant sum frequency $|\tilde{\beta}|$ can be increased by functionalizing these molecules with suitable “push-pull” chromophores.^{34,40}

SFG in the presence of a dc-electric field. As the sum-frequency signal is proportional to the square of the

enantiomeric concentration difference, SFG can in general not distinguish between optical isomers. However, Buckingham and Fischer have predicted that the application of a static electric field to a SFG process allows the enantiomers of a chiral solute to be distinguished and their absolute configuration to be determined.⁴¹ The static field gives rise to an electric-field induced contribution to coherent sum-frequency generation. This is an achiral electric-dipolar third-order contribution, such that the combined sum-frequency polarization along x is given by

$$P_x(\omega_1 + \omega_2) = \varepsilon_0 \left[\underbrace{\chi^{(2)} E_y(\omega_1) E_z(\omega_2)}_{\text{chiral}} + \underbrace{\chi^{(3)} E_y(\omega_1) E_y(\omega_2) E_x(0)}_{\text{achiral}} \right], \quad (31)$$

where we assume that the ω_1 beam travels along the z direction and has its electric field vector oscillating along y , and the ω_2 beam to be plane polarized in the yz plane (see Fig. 3). The SFG signal is $\sim |\vec{P}(\omega_1 + \omega_2)|^2$, and the cross-term between the chiral $\chi^{(2)}$ and the achiral electric-field induced $\chi^{(3)}$ gives a contribution to the sum-frequency intensity that is linear in the static field, which is linear in $\chi^{(2)}$:

$$\text{SFG}(E) \propto \chi^{(2)} * \chi^{(3)} E(0), \quad (32)$$

where we denote the contribution to the intensity at the sum frequency that is linear in the static field by $\text{SFG}(E)$. Thus the absolute sign of the pseudoscalar $\chi^{(2)}$ (and hence $\tilde{\beta}$) can be obtained. It, in turn, is needed to determine the absolute configuration of the chiral solutes in the optically active liquid.

Fischer et al. have recently observed the effect in solutions of 1,1'-bi-2-naphthol and have demonstrated that it allows nonlinear optical sum-frequency generation to be used to determine the absolute configuration of a chiral solute via an electric-dipolar optical process.²⁸ Figure 3 shows that the $\text{SFG}(E)$ signals depend linearly on the

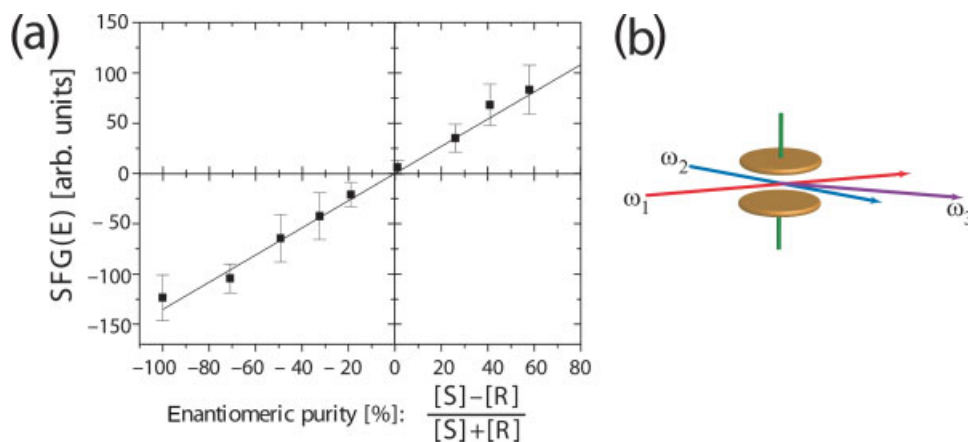


Fig. 3. (a) $\text{SFG}(E)$ signals measured as a function of the fractional concentration difference in R -(+)- and S -(−)-1,1'-bi-2-naphthol in tetrahydrofuran. (b) SFG beam geometry. (Adapted from ref. 28).

strength of the dc field and that they change sign with the enantiomer.

Vibrational SFG. Sum-frequency generation can probe electronic as well as vibrational transitions. If one of the lasers is tunable in the infrared, SFG may be used to record the vibrational spectrum of a chiral molecule. SFG vibrational spectra from neat limonene in the region of the CH-stretch have been reported by Shen and co-workers.^{23,42} The strength of the chiral CH-stretch modes in the limonene solutions $|\chi^{(2)}|$ was reported to be about 3 orders of magnitude smaller than a typical achiral stretch.²³ Chiral spectra are measured with p-polarized input beams and a s-polarized sum-frequency beam, and with one s- and one p-polarized incident beam and a p-polarized sum-frequency. The liquids from the two enantiomers can be distinguished if beam polarizations are used that permit the observation of mixed chiral/achiral SFG.²³

The scattering amplitude for vibrational SFG in a liquid is proportional to the (generally weak) antisymmetric Raman tensor associated with the vibrational mode which is probed by the infrared resonance. Belkin et al. have shown that the antisymmetric part of the Raman tensor can become comparable in strength to the symmetric part under conditions of double-resonance (vibrational and electronic),⁴³ and strong enhancement in doubly resonant SFG was recently observed in the vibrational spectrum of BN in solution and on a surface.²⁷

Time-resolved vibrational SFG optical activity measurements with circularly polarized infrared light have been proposed.⁴⁴

SURFACE NONLINEAR OPTICS

Second harmonic generation (SHG) is a surface specific spectroscopy that probes molecular order at surfaces and interfaces, e.g., the liquid/air interface.^{45,46} In SHG, a lightwave from a laser is incident on a surface or an interface at a fixed angle with respect to the surface normal. The incident field at the frequency ω induces dipole moments that oscillate at 2ω . Coherent addition of these moments from the surface leads to a macroscopic polarization

$$\vec{P}(2\omega) = \epsilon_0 \vec{\chi}^{(2)}(\omega + \omega) \vec{E}(\omega) \vec{E}(\omega), \quad (33)$$

which radiates a lightwave at the second harmonic (2ω) in the specular direction. The intrinsic surface specificity of SHG originates from the symmetry breaking that occurs at an interface. Whereas $\vec{\chi}^{(2)}(\omega + \omega)$ vanishes in the bulk of isotropic media, it is nonzero at surfaces and interfaces where the molecules may adopt a preferred orientation. Compared to linear optical spectroscopies, SHG can probe a single layer of molecules on a surface with little background signal from the bulk. Furthermore, as SHG is a nonlinear optical process, it relies on several parameters, such as the directions or the polarizations of the incoming light beams, and is therefore experimentally more versatile than a linear optical technique.

In 1993, Hicks and co-workers discovered that circular intensity differences in SHG are a probe of surface chirality.²⁰ The application of SHG to the study of chiral molecules has been pioneered by Hicks and co-workers^{20,47} on 1,1'-bi-2-naphthol (BN) and by Persoons and co-workers⁴⁸ on a functionalized poly(isocyanide) polymer. Numerous studies on chiral-surface SHG have since appeared in the literature, and we review some of them here.

In the case of SHG from a surface layer of chiral molecules, symmetry breaking is 2-fold: First, the interface breaks centrosymmetry such that surface SHG may occur, and second, the symmetry breaking in chiral molecules gives rise to additional contributions to the SHG signal. Both of these features contribute to surface SHG from chiral molecules. As described in the theoretical background material, SHG can be observed from an achiral surface as well as a chiral surface. Even for a chiral surface, the dominant signals can be electric-dipolar (or "local")

$$\vec{P}^{(2)}(2\omega) = \epsilon_0 \vec{\chi}^{eee} E(\omega) E(\omega), \quad (34)$$

where we label the susceptibility by the operators that enter its quantum mechanical expression (here a product of three electric-dipole (e) transition moments). In contrast to linear optical activity phenomena, no magnetic dipolar or electric quadrupolar ("nonlocal") contributions are required in SHG in order to observe a chiral optical response. In this case, surface SHG probes chirality, similar to sum-frequency generation from the bulk of a liquid, via susceptibility tensor elements that depend on the three orthogonal spatial directions "XYZ." We discuss how SHG can be used to determine the origin of a molecule's optical activity, and we shall see that the chiral SHG response for certain molecules is determined by electric-dipolar (local) susceptibilities and for others by magnetic-dipolar (nonlocal) susceptibilities.

Chiral SHG: experimental setup. The basic experimental geometry is depicted in Figure 4. The beam

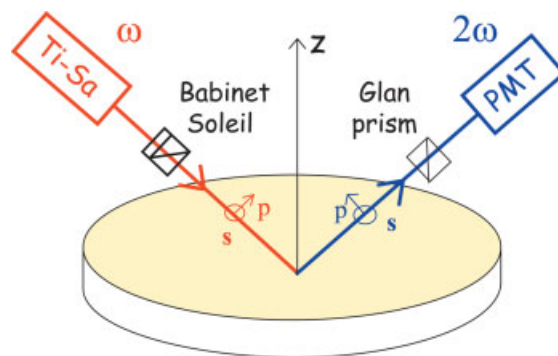


Fig. 4. Surface SHG geometry. The surface normal is the Z direction in the laboratory frame. The angle of incidence is constant at 45°.

polarizations are controlled either by polarizers, waveplates, or Babinet–Soleil compensators. The lightwave at the second harmonic is typically detected with a photomultiplier tube. Its intensity is proportional to $|\vec{P}(2\omega)|^2$. Three types of experiments have been devised to study the response of a chiral surface that is rotationally invariant with respect to the surface normal (C_∞ symmetry). In SHG optical rotatory dispersion (SHG-ORD),^g the incident beam is p-polarized^h and the detection of any “rotated” s-polarized^h polarization component at the second-harmonic indicates the presence of chiral molecules on the surface. Similarly, a difference in the SHG intensity as the circularity of a circularly polarized incident beam is reversed is a signature of chiral molecules. This difference in SHG conversion efficiency is termed “second-harmonic generation circular difference” (SHG-CD).^g A second-harmonic generation linear difference (SHG-LD) measurement consists of measuring the SHG intensity for the incident fundamental beam polarized at $\pm 45^\circ$ with respect to the plane of incidence.⁴⁹ Here again, the observation of an intensity difference is a sign of chiral molecules. In SHG-CD and SHG-LD experiments, the polarization states of the incident light can be continuously modulated with a rotating quarter-wave or half-wave plate, respectively, which dramatically improves the signal-to-noise ratio in these measurements.

The intensity differences in SHG experiments on chiral surfaces can be relatively much larger than commonly observed in typical linear optical ORD or CD experiments. For example, Hicks et al. measured SHG circular intensity differences of order unity from a monolayer of the R-enantiomer of BN,⁵⁰ while in linear optics the difference between the left and right circularly polarized absorptivity divided by their sum is typically 10^{-3} .⁹ Hicks and co-workers also showed that the origin of the SHG signals from BN can be explained within the electric-dipole approximation, as their experimental data agreed well with a theoretical calculation of the electric-dipolar nonlinear surface susceptibility.³⁵ However, it is reasonable to expect that SHG signals from (certain) chiral molecules will, in general, also contain magnetic dipolar (and electric quadrupolar) contributions.⁵¹

Local and nonlocal contributions to SHG. We show that magnetic-dipolar and electric-quadrupolar contributions are indeed required to understand SHG in some chiral molecules. Nonlocal susceptibilities should thus be included in the SHG response. In general, magnetic-dipolar as well as electric-quadrupolar terms ought to be considered separately.^{8,52} Instead, one usually writes all the nonlocal terms collectively as a single, generalized “magnetic contribution.”⁴⁸ This is justified, as it is not possible to experimentally distinguish between the

magnetic-dipolar and the electric-quadrupolar terms in a typical surface second-harmonic experiment.³⁷ The total polarization is then expressed as

$$\vec{P}^{(2)}(2\omega) = \varepsilon_0 \vec{\chi}^{eee} \vec{E}(\omega) \vec{E}(\omega) + \varepsilon_0 \vec{\chi}^{eem} \vec{E}(\omega) \vec{B}(\omega), \quad (35)$$

and it is necessary to introduce the nonlinear magnetization

$$\vec{M}^{(2)}(2\omega) = \varepsilon_0 \vec{\chi}^{mee} \vec{E}(\omega) \vec{E}(\omega). \quad (36)$$

The nonlocal $\vec{\chi}^{mee}$ and $\vec{\chi}^{eem}$ susceptibilities are also third-rank tensors, but their symmetry differs from the local, electric-dipolar susceptibility, due to the presence of a magnetic-dipole transition moment (m) in place of an electric-dipole transition moment (e). The nonzero components of these susceptibilities for achiral and for chiral surfaces can be found in reference 52. In order to establish the extent to which the nonlocal susceptibilities contribute to the chiral SHG signals, one needs to devise an experiment that can, on the one hand, distinguish between local and nonlocal signals and, on the other hand, between chiral and achiral signals. Should the local (electric-dipolar) contributions dominate, then a counter-propagating beam geometry can be used to separate the chiral from the achiral contributions.⁵³ However, to some extent the various contributions remain mixed.

It is possible to separate the achiral and chiral contributions by examining the field at the second harmonic if it is written in the following form:

$$\vec{E}_{s,p}(2\omega) = f_{s,p} \vec{E}_p^2(\omega) + g_{s,p} \vec{E}_s^2(\omega) + h_{s,p} \vec{E}_p(\omega) \vec{E}_s(\omega). \quad (37)$$

The advantage of this formulation is that the parameters f_p , g_p , h_s are functions of only the *achiral* components whereas f_s , g_s , h_p depend exclusively on *chiral* susceptibilities. Exact expressions for these coefficients as a function of the susceptibility tensors can be found in reference 48. Note that these coefficients are complex-valued and that each coefficient contains electric as well as magnetic contributions—with the exception of g_s which involves only magnetic terms. Plotting the SHG intensity as a function of the waveplate angle allows one to extract the f , g , and h coefficients.⁵⁴ An example of such a measurement is given in Figure 5. Fitting of these curves (for explicit fitting formulas, see Schanne-Klein et al.⁵⁵) yields the real and imaginary parts of the coefficients. These measurements only reveal the relative phase of the various coefficients and are therefore not quite sufficient to unambiguously separate the electric and the magnetic contributions in the surface SHG signal. However, achiral contributions are generally electric-dipolar, such that the phase of the achiral coefficients, e.g., f_p , g_p , h_s , can serve as a reference. It is then possible to separate the electric from the magnetic contributions in the chiral coefficients: those in phase with the achiral coefficients are electric dipolar, and those in quadrature correspond to the magnetic

^gSHG-ORD and SHG-CD are unrelated to “optical rotatory dispersion” and “circular dichroism” in linear optics (see “Theoretical Background”).

^hThe electric field vector is orthogonal to the plane of incidence for s-polarized light and parallel to the plane of incidence in p-polarized light.

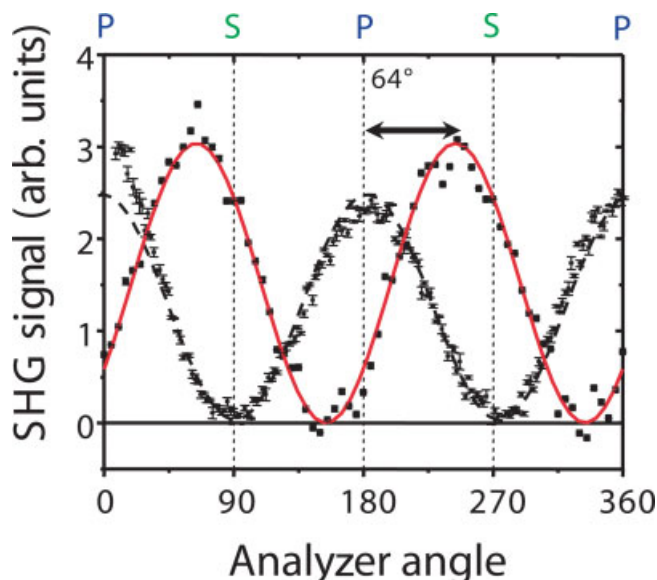


Fig. 5. Second-harmonic generation from a surface of chiral stilbene (small squares—black dashed line) and of a Tröger's base (large squares—red solid line) as a function of the analyzer angle. No polarization rotation is observable for the stilbene, whereas a 64° rotation is measured for the Tröger's base.

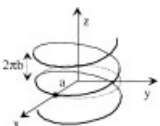
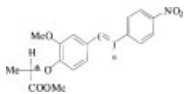
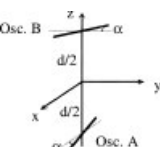

terms. The phase relationship is expected to hold even on resonance, provided the electric- and magnetic-dipolar transitions involve the same energy levels.

Molecular origin of chiral SHG. The question whether magnetic (nonlocal) contributions to surface SHG are measurable, arose early on. Byers et al.³⁵ showed that their results on 1,1'-bi-2-naphthol could be fully explained within the electric-dipole approximation, whereas Kauranen et al. showed that magnetic terms were essential to account for their measurements on a polymer (poly-isocyanide) film.⁵⁶ The presence of magnetic con-

tributions was also clearly observed in a SHG study of chiral polythiophene, where a nonzero g_s was measured.⁵⁶ This finding was confirmed by Schanne-Klein et al., who also measured a nonzero g_s in a pentamethinium salt.⁵⁷

These findings do not contradict each other if one considers the molecular basis for optical activity in these molecules and its implications for second-order nonlinear optics. Two principal mechanisms are responsible for a chiral molecule's optical activity⁵⁷: (i) a one-electron mechanism in which the electric and the magnetic transitions are mixed on the same chromophore due to its asymmetric environment; and (ii) a coupled-oscillator mechanism, in which two electric-dipole-allowed transitions belonging to two separate chromophores in the molecule are asymmetrically coupled. Hache et al.³⁷ have used a classical model to calculate surface SHG signals and have shown that the dominant chiral surface susceptibilities have a magnetic origin for molecules that exhibit "one-electron optical activity," whereas for molecules with "coupled-oscillator optical activity" the electric contributions dominate. These calculations also explain the experimental findings: 1,1'-bi-2-naphthol, studied by Hicks et al., shows coupled-oscillator chirality, and it is therefore not necessary to consider nonlocal (magnetic) contributions to SHG. This has been confirmed by Fischer et al., who used SFG to discriminate between the nonlocal and the local response and have shown that the latter clearly dominates in 1,1'-bi-2-naphthol.²⁶ Nonlocal susceptibilities are, however, essential in order to explain the results obtained with the molecules studied by Kauranen et al. and Schanne-Klein et al. which pertain to the one-electron case. Interestingly, further conclusions can be drawn from the model calculations (see Table 2). When examining the signal obtained in surface SHG experiments, one can see that SHG-ORD and SHG-LD will give a specific chiral signal only if the second-order susceptibility is electric-dipolar, and these two experimental configurations are thus not sufficient to unambiguously detect the presence of chiral molecules on a surface. SHG-CD gives a chiral signal irrespective of the mechanism. The mecha-

TABLE 2. Second-order nonlinear optical response modeled by a one-electron mechanism (represented by a helix) and a coupled-oscillator mechanism (represented by two anharmonic oscillators)³⁷

Model	Example	Relevant parameters	Expected effects
		$f_p, g_p,$ and h_s (achiral) = electric dipolar $f_s, g_s,$ and h_p (chiral) = magnetic dipolar	SHG-CD
		$f_p, g_p,$ and h_s (achiral) = electric dipolar + electric quadrupolar + magnetic dipolar $f_s, g_s,$ and h_p (chiral) = electric dipolar	SHG-CD + SHG-LD, SHG-ORD

Respective examples are from experiments on a chiral stilbene⁵⁹ and a Tröger's base.⁵⁸

nism of a chiral molecule's optical activity may therefore be determined by examining both SHG-ORD and SHG-LD experiments. This is not possible in linear optics, which demonstrates the potential of nonlinear optical spectroscopies to distinguish between "one-electron" and "coupled-oscillator" chirality. The mechanism of optical activity in an acridine-substituted Tröger's base⁵⁸ and a chiral stilbene⁵⁹ have been determined with SHG measurements (see Fig. 6). A large rotation of the SHG polarization has been recorded for the Tröger's base, whereas no rotation could be observed in the chiral stilbene. Hache et al. report a SHG rotation of 64° in the Tröger's base, which is the largest rotation observed to date in a surface SHG experiment. It is instructive to compare SHG-ORD with conventional, linear optical rotatory dispersion (ORD). The chiral surface SHG signals originate from a thin film of chiral molecules. The same number of molecules would give rise to an ORD angle that is far below the limit of detection. We estimate that the rotation measured in the film is 6 orders of magnitude larger in the surface SHG experiment than it would be in conventional ORD. This demonstrates the excellent sensitivity of surface SHG to detect chiral molecules.

All of the above-mentioned capabilities of surface SHG measurements on chiral molecules require that the

surface be symmetric with respect to the surface normal. Should the distribution of molecules be anisotropic within the surface plane (i.e., not C_∞), then circular and linear intensity differences can also be observed from achiral molecules, as has been shown by Verbiest and colleagues.^{60,61} Electric-dipole-allowed SHG (and SFG) from achiral molecules—that are arranged such that the surface is chiral—have been studied.^{62,63} A careful tensor analysis of the response from anisotropic chiral films has shown that it is nevertheless possible to separate the effects due to anisotropy from those due to chiral molecules.^{64,65}

The molecular aspects of chiral second-order nonlinear optical spectroscopies (SHG and SFG) have also been discussed in a recent mini-review by Simpson.⁶⁶

Sum-frequency generation from chiral surfaces. Surface second-order optical measurements are not restricted to SHG. Sum-frequency generation (SFG) is equally versatile.⁶² It has the advantage that the incident frequencies can be tuned independently. Shen and co-workers measured the SFG spectrum of a monolayer of BN on water between 310 and 360 nm with a laser beam at $1.06\ \mu\text{m}$ and another beam tunable from 450 to 550 nm.⁶⁷ The sum frequency was resonant with the lowest-lying absorption of BN with rich spectral content, and the polarization of the SFG provided additional information on the molecules' orientation.⁶⁷ Should one of the lasers be tunable in the infrared, then vibrational sum-frequency spectra can be recorded. Large enhancements of the chiral response have been reported in recent doubly-resonant experiments.²⁷ These have allowed the vibrational sum-frequency spectrum of a BN monolayer to be recorded.²⁷

Applications of chiral surface spectroscopies: nonlinear optics and proteins. Apart from the fundamental questions addressing the molecular mechanism that underlie surface SHG in a number of chiral molecules, several applications of surface SHG have recently been reported.

Taking advantage of the fact that the second-order susceptibility changes sign with the opposite enantiomer of a chiral molecule, Busson et al. have demonstrated quasi-phase matching in a structure composed of alternating stacks of helicenebisquinone.⁶⁸ Interesting applications may arise when chiral molecules are used in materials for nonlinear optical frequency conversion. Research in this direction is pursued in a number of laboratories.^{69,70}

Chiral-surface SHG has also been observed from molecules of biological interest. A measurement on a dipeptide (*tert*-butyloxycarbonyl-tryptophan-tryptophan) at the air/water interface has been reported.⁷¹ SHG-CD and SHG-ORD measurements revealed the handedness of the dipeptide conformation. The handedness was assigned to a twisted conformation of the two tryptophans. SHG-CD has also been used, together with a surface-enhanced resonance Raman study, to monitor the oxidation state of

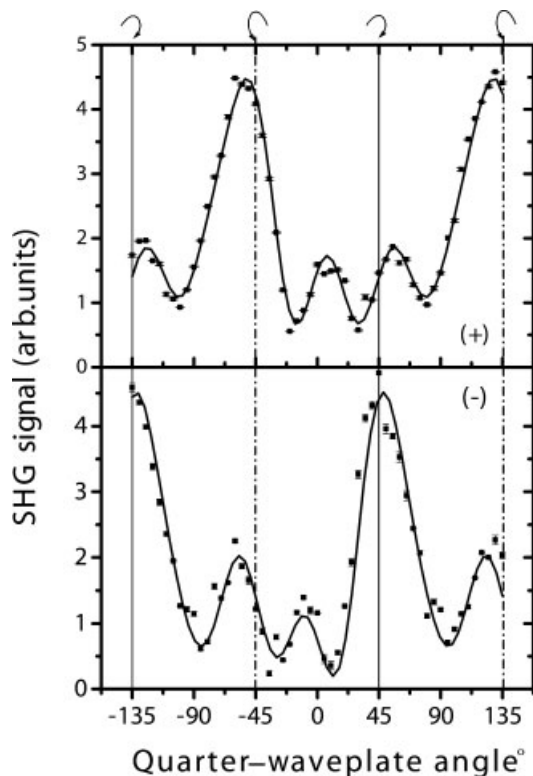


Fig. 6. SFG-CD: *p*-polarized component of the SHG signal from a surface of Tröger's base as a function of the rotation angle of a quarter-waveplate. (Top) (+)-Enantiomer; (bottom) (–)-enantiomer. Arrows at $+45^\circ$ and -135° indicate that the polarization of the fundamental laser beam is right circularly polarized, and correspondingly arrows at -45° and $+135^\circ$ that it is left circularly polarized. The lines are theoretical fits of the f_p , g_p , and h_p functions to the data.

cytochrome *c* adsorbed on model membranes surfaces.⁷² SHG-CD was shown to be a particularly sensitive probe of the redox state of the heme group, which is known to be essential for the electron transfer process that occurs in cytochrome *c*. Simpson and co-workers used chiral SHG experiments to observe the dynamics of protein binding (bovine serum albumin) to a surface.⁷³ Their experimental results are shown in Figure 7. Recently, chiral SHG signals from the peptide melittin allowed Conboy et al. to detect its binding to a lipid bilayer.⁵³ The same group has also developed a chirality-specific form of SHG microscopy which used a counterpropagating geometry⁵³ to image a patterned surface.⁷⁴

THIRD-ORDER NONLINEAR CHIROPTICAL EFFECTS IN A LIQUID

Thus far we have discussed nonlinear optical effects which are quadratic in the optical fields and which give rise to the generation of light at a new frequency that is different from that of the incident laser. We now turn

to those nonlinear optical effects that can modify the optical properties of an optically active liquid. As shown in the theoretical background material, this may occur at third order, where the optical response depends on the cube of the optical fields and has a component that oscillates at the frequency of the laser. The so-called “optical Kerr effect” occurs in any medium and gives rise to a nonlinear contribution to the refractive index. It depends on the (achiral) hyperpolarizability $\vec{\gamma}$ (cf. eq. (15)), and we can write the corresponding macroscopic polarization as

$$\vec{P}(\omega) = \varepsilon_0 \vec{\chi}^{eee}(\omega - \omega + \omega) |\vec{E}(\omega)|^2 \vec{E}(\omega), \quad (38)$$

where we have indicated that the third-order susceptibility is electric-dipolar, and where we have given its frequency argument $\omega - \omega + \omega$ (which is $= \omega$). Apart from the intensity-dependent refractive index (eq. (17)), many important nonlinear optical phenomena, including self-focusing, self-phase modulation, and two-photon absorption, are directly related to the susceptibility in eq. (38).³

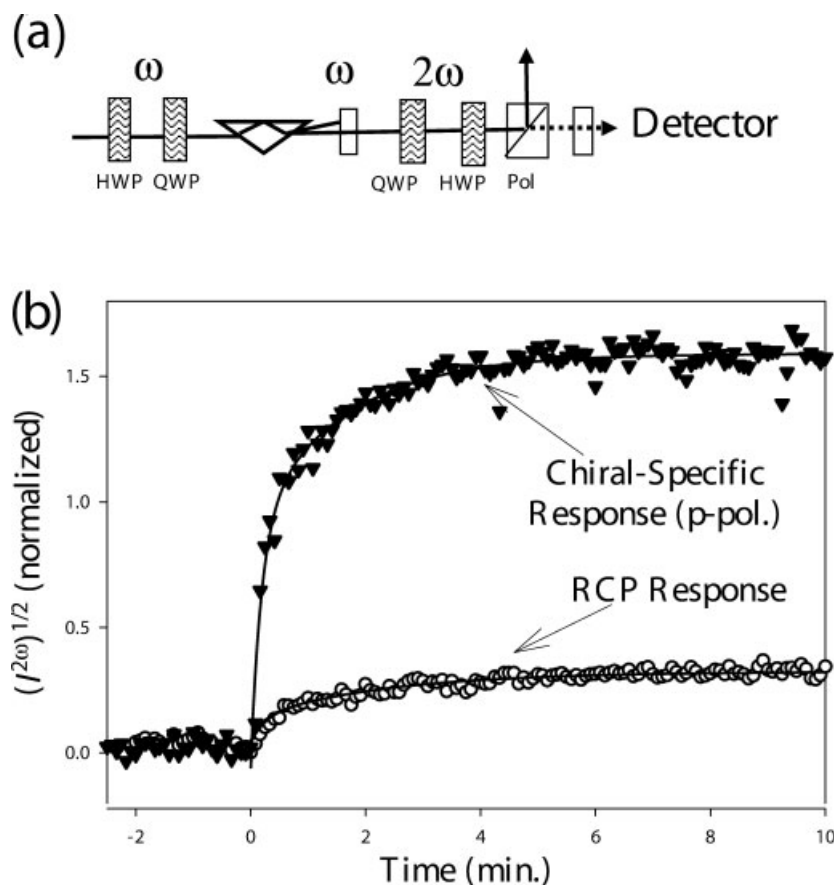


Fig. 7. Chiral-specific approach for label-free measurements of bovine serum albumin (BSA) binding using a rhodamine dye as a local probe for interfacial chirality. In the absence of the protein, the SHG generated at the interface was suppressed by passing the beam through an appropriately oriented quarter-wave plate (QWP)/half-wave plate (HWP)/polarizer (Pol) combination (a). Upon exposure to an aqueous protein solution, the change in the polarization state of the SHG (presumably, through changes in the orientation distribution of the rhodamine dye) resulted in an SHG signal scaling with the square of the surface protein density (b). Solid lines in (b) are fits of the data to exponential rises to maxima. In the upper curve (corresponding to s-polarized detection with a p-polarized incident beam), the polarization combination used exclusively probes the chiral-specific SHG response of the interface. (Figure provided by Prof. G.J. Simpson, see also reference 73).

Laser beams with two different frequency components can also interact in a medium via a third-order susceptibility and give rise to frequency conversion processes, or modify each other's refractive index, e.g., $\omega_1 - \omega_2 + \omega_2$. The latter also describes pump–probe experiments, where the fields at ω_1 and ω_2 are short pulses that are incident with variable time delays in order to observe any effect resulting from the induced polarization as a function of the time between the pulses.³

We now discuss how the optical Kerr effect and all the related achiral nonlinear optical phenomena may become specific to chiral molecules.

Nonlinear optical activity. Chiroptical effects at third-order have first been discussed by Akhmanov⁷⁵ and Barron⁷⁶ in the early years of nonlinear optics, and aspects of the theory have since been developed further.^{77,78} Optical activity arises in the nonlinear response if one goes beyond the electric dipole approximation in eq. (38). Instead of the electric-dipole susceptibility χ^{eeee} , one needs to consider nonlocal susceptibilities that contain a magnetic-dipolar or electric-quadrupolar transition in place of an electric-dipole transition (e), such as χ^{eem} ($\omega - \omega + \omega$) and similar expressions for the electric-quadrupolar susceptibilities. A rigorous introduction of these susceptibilities and a discussion of their properties can be found in the book by Svirko and Zheludev.⁵¹ From the phenomenological discussion in the introductory material, it follows that one expects nonlinear optical activity effects in refraction and absorption according to eq. (18)

$$n^{\pm} \approx (n_0 + n_2 I) \pm (g_0 + g_2 I),$$

where the nonlinear optical activity index, g_2 , gives rise to nonlinear optical rotatory dispersion (NLORD) and nonlinear circular dichroism (NLCD), respectively.

There are only two experimental studies of NLORD to date: a light-induced optical rotation due to thermal effects,⁷⁹ and a nonlinear optical rotation study on uridine and sucrose by Cameron and Tabisz.⁸⁰ The first experimental evidence of NLCD has recently been obtained by Mesnil and Hache from solutions of ruthenium(II) tris(bipyridyl) (RuTB), where, in agreement with theoretical predictions, an intensity-dependent contribution to the circular dichroism spectrum has been observed.^{81,82} As required, the NLCD spectrum changed sign with the enantiomer and vanished for the racemic mixture. Extension of these measurements to a pump–probe configuration has recently been reported.⁸³ Two independently tunable lasers have been used to simultaneously acquire both linear and nonlinear CD (and absorption) spectra of RuTB (see Fig. 8), demonstrating the potential of this technique for spectroscopic applications.

Nonlinear optical activity is expected to be widely used in the future, and a modified Z-scan technique has recently been proposed that allows nonlinear chiroptical phenomena to be studied with a simple experimental setup.⁸⁴ Many more nonlinear techniques will undoubtedly be

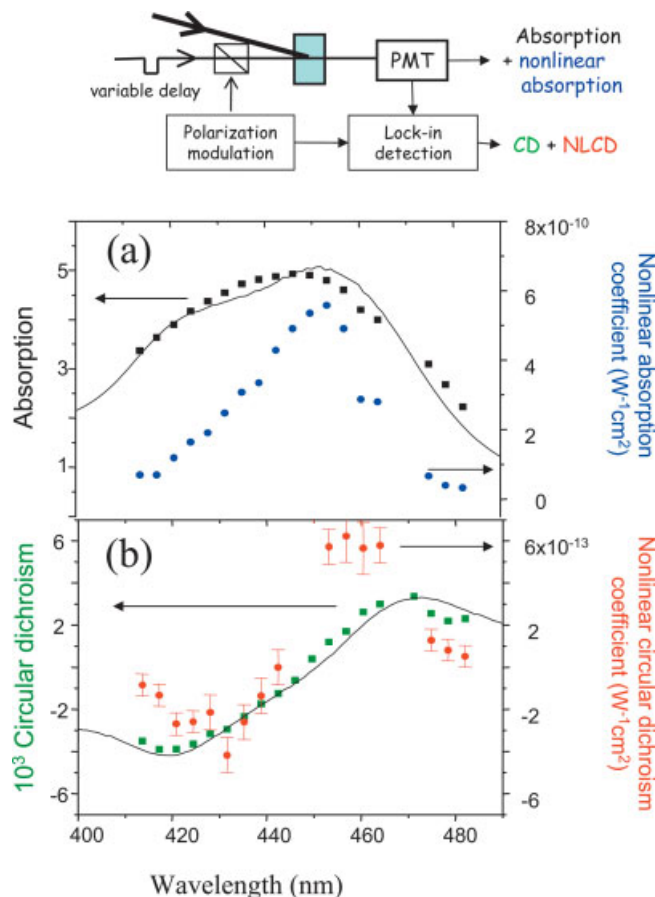


Fig. 8. (a) Linear (black squares) and nonlinear (blue dots) absorption and, (b) linear (green squares) and nonlinear (red dots) CD measurements in a pump–probe experiment as a function of the probe wavelength. The wavelength of the pump is 465 nm. The linear spectra are measured in a 2-mm-thick cuvette; the nonlinear coefficients are given in absolute units (W⁻¹ cm²). The solid lines are the spectra measured using spectrophotometers.

developed in the future, as exemplified by a recent theoretical study of two-dimensional circularly polarized pump–probe spectroscopy.⁸⁵

Nonlinear chiroptical properties could yield applications for signal processing. One study reported experiments on an optical switch based on light-induced isomerization.⁸⁶ Recently, use of nonlinear chiral photonic bandgap structures for all-optical switching was proposed.⁸⁷

Investigation of biomolecules by time-resolved chiroptical techniques. In one form of pump–probe experiments, an intense laser pulse is used to bring molecules into an excited (electronic or vibrational) state. Evolution of the excited molecules is then monitored by a second, weaker pulse which probes the state of the molecules. Most often, it is the absorption of the probe which gives the relevant information. Measurements are carried out as a function of the time delay between the two pulses, and the time resolution is a function of the pulse duration. This popular technique permits resolution of processes at ultrafast time scales. Extension of these techniques to

chiral molecules and more specifically to biomolecules is indeed appealing because it allows one to probe dynamic stereochemical properties. Optical activity is often a measure of global structure in biomolecules and can therefore provide information that is not accessible to other pump–probe techniques.

The most advanced applications of chiral pump–probe spectroscopy concern time-resolved circular dichroism studies which have been used to follow the structural dynamics of protein conformation.⁸⁸ Pump-induced *linear* CD measurements (i.e., linear optical activity and not NLCD) have been reported of the photolysis of carbon-monoxymyoglobin at nanosecond⁸⁹ and picosecond⁹⁰ time scales, and recently sub-100-picosecond CD dynamics has been observed in the same protein.⁹¹ The observed conformational changes upon photolysis of CO from myoglobin have been interpreted with the help of CD calculations based on a classical polarizability theory.⁹²

Given the numerous applications of electronic CD spectroscopy for secondary structure determination of proteins, it is expected that time-resolved CD will play an important role in the elucidation of ultrafast protein folding and structural dynamics.

Coherent Raman optical activity. Nonlinear extensions of natural optical activity phenomena are not restricted to optical rotation and circular dichroism. Nonlinear optical analogs of Raman optical activity (ROA) have also been considered and their theory has been discussed.^{93,94} ROA measures a small difference in the vibrational Raman spectrum for left- and right-circularly polarized incident light.^{95,96} Although Raman optical activity is now routinely used to study chiral (bio)molecules in aqueous solution,⁹⁵ it is an incoherent spectroscopy and the signals are thus weak. Spontaneous Raman scattering can easily be masked by light emitted from competing processes such as fluorescence. Nonlinear Raman spectroscopies could be of value in the study of vibrational optical activity, as they make it possible to probe Raman resonances through coherent rather than incoherent scattering.⁹⁴ The signal strength in nonlinear Raman spectroscopies, such as coherent anti-Stokes Raman scattering (CARS) and Raman-induced Kerr effect spectroscopy (RIKES), is therefore typically at least 3 orders of magnitude larger than in spontaneous Raman scattering.⁹⁷ Nonlinear Raman spectroscopy should make it possible to eliminate interference from fluorescence, and to obtain previously unavailable temporal information about a molecule's vibrations. Nonlinear Raman optical activity is described by nonlocal third-order susceptibilities of the form $\chi_{eeem}^{(3)}(\omega_1 - \omega_2 + \omega_1)$.^{93,94} In CARS, the laser at ω_2 is tuned, and when the difference in angular frequencies $\omega_1 - \omega_2$ is proportional to a vibrational energy $\hbar\omega_{\text{vib}}$, a resonantly enhanced signal is observed at $\omega_1 + \omega_{\text{vib}}$. To our knowledge, there is only one report of a successful nonlinear Raman optical activity measurement from a chiral liquid to date. Spiegel and Schneider have observed Raman optical activity with CARS in a liquid of (+)-*trans*-pinane and report chiral signals that are $\sim 10^{-3}$ of

the conventional electric-dipolar CARS intensity.⁹⁸ They used a band-shape analysis of three ROA bands between 750 and 870 cm^{-1} in the CARS spectrum and report nonlinear ROA spectra in excellent agreement with theory.⁹⁸ The nonlinear ROA effects are predicted to be much larger near electronic resonance.

CHIRAL SPECTROSCOPIES AT FOURTH-ORDER

Similar to linear optical activity, the spectroscopies at third-order are characterized by signals that are primarily achiral and, in the case of optically active liquids, may have an additional, small chirality-specific contribution. The latter is observed as an intensity difference signal that requires accurate polarization modulation or the measurement of small angles of rotation. This is in contrast to sum-frequency generation at second order, which is electric-dipolar and is essentially background-free. Extension of third-order processes in optically active liquids to fourth-order, as first proposed by Koroteev,⁹⁹ would again allow for the observation of a background-free, electric-dipolar chiral signal. Although $\chi^{(4)}$ is in general much weaker than $\chi^{(2)}$, a fourth-order process would have the distinct advantage that it can be realized in a phase-matched geometry. The nonlinear polarization of a fourth-order process has a quartic dependence on the electric fields and is—in a liquid—given by

$$\vec{P}(3\omega_1 - \omega_2) = \epsilon_0 \chi^{(4)}(3\omega_1 - \omega_2) * (\vec{E}(\omega_1) \times \vec{E}(\omega_2))(\vec{E}(\omega_1) \cdot \vec{E}(\omega_2)), \quad (39)$$

for the incident waves at ω_1 and ω_2 .^{99,100} There is an experimental report of such a process in liquids. Using two noncollinear frequency-degenerate beams ($\omega_1 = \omega_2$), Shkurinov et al. report the observation of weak signals that exhibited polarization characteristics as predicted by eq. (39).¹⁰¹ We note that recent attempts to reproduce earlier reports of SFG from arabinose^{101,102} have not been successful and have shown that the $\chi^{(2)}$ of arabinose is much weaker than previously thought.^{22,24}

A new coherent chiral Raman spectroscopy, that arises when $3\omega_1 - \omega_2$ in eq. (39) is equal to the angular frequency of a vibration, has been proposed by Koroteev who gave it the acronym “BioCARS” to indicate that this spectroscopy would constitute an extension of CARS to chirality, and hence biology.¹⁰³ BioCARS would exclusively probe chiral Raman vibrations that are simultaneously Raman and hyper-Raman active.^{103,104} The spectroscopy does not require the use of circularly polarized light to detect chirality and would allow for a complete rejection of fluorescence, but it could not distinguish between optical isomers. BioCARS has not yet been observed. Apart from the inherent weakness of a nonlinear optical susceptibility responsible for BioCARS, fourth-order processes (and SFG) in liquids are weak as they require a noncollinear beam geometry (due to the vector cross product in eqs.

(22) and (39)) which further reduces the interaction length. The use of a waveguide, as suggested by Zheltikov *et al.*, may constitute a promising alternative as it would allow for a collinear beam geometry and therefore a more efficient implementation of BioCARS.¹⁰⁵

CONCLUSION AND OUTLOOK

The principles of nonlinear optical probes of chiral molecules in solution and on surfaces have been reviewed, and several selected applications of the various spectroscopies have been presented. Whereas a few of the nonlinear optical processes discussed in this review have not yet, or only recently, been observed, the majority of nonlinear spectroscopies that can be specific to chiral molecules, including second-harmonic generation, sum-frequency generation, and, to some extent, nonlinear optical activity, are now well understood. The nonlinear techniques are not as general and efficient as conventional linear optical activity measurements—they require pulsed lasers and often some form of resonance enhancement—but nonlinear processes can reveal aspects of molecular chirality not accessible to linear optics. We have shown that nonlinear optics can be more sensitive than conventional optical activity probes. A monolayer of chiral molecules may for instance be studied by second-harmonic and sum-frequency generation at surfaces with little contribution from the bulk of the liquid. The corresponding chiral nonlinear optical observables can be many orders of magnitude larger than they would be in typical linear optical ORD or CD experiments. Second-order processes can also be used to experimentally determine whether a molecule's optical activity is primarily due to a one-electron or due to a coupled-oscillator mechanism. Nonlinear optical activity measures intensity-dependent contributions to optical rotation and circular dichroism and makes it possible to study the conformation of chiral molecules at ultrafast time scales. Some nonlinear optical phenomena, such as sum-frequency generation (and BioCARS) in optically active liquids, have no direct analogue in linear optics. They arise in the absence of magnetic-dipole transitions and without any background signals, so that the frequency conversion in itself is a measure of a solution's enantiomeric excess.

Novel applications of nonlinear chiral spectroscopies to the study of biological interfaces, the determination of absolute configuration, and protein dynamics have recently been reported, and we expect that nonlinear optical spectroscopies will become important tools in the investigation of molecular chirality.

Note added in proof: The following papers have appeared after completion of this review: A paper by Wang *et al.* that reports the observation of chiral vibrational SFG spectra of proteins at the solid/liquid interface away from electronic resonance.¹⁰⁶ A SHG study of polypeptide α -helices at the air water interface.¹⁰⁷ A theoretical paper that examines chiral third-order spectroscopies.¹⁰⁸

ACKNOWLEDGMENTS

The authors thank Prof. G.J. Simpson for providing Figure 7. P.F. is grateful for a Junior Research Fellowship from the Rowland Institute at Harvard.

LITERATURE CITED

- Lowry TM. Optical rotatory power. New York: Dover; 1964. 483 p.
- Wagnière GH. Linear and nonlinear optical properties of molecules. Basel: VCH; 1993. 195 p.
- Butcher PN, Cotter D (editors). The elements of nonlinear optics. Cambridge, England: Cambridge University Press; 1990. 344 p.
- Boyd RW. Nonlinear optics. London: Academic Press; 1992. 439 p.
- Sioncke S, Verbiest T, Persoons A. Second-order nonlinear optical properties of chiral materials. *Mater Sci Eng R* 2003;42(5–6):115–155.
- Pu L. The study of chiral conjugated polymers. *Acta Polym* 1997;48(4):116–141.
- Dhenaut C, Ledoux I, Samuel IDW, Zyss J, Bourgault M, Lebozec H. Chiral metal-complexes with large octupolar optical nonlinearities. *Nature* 1995;374(6520):339–342.
- Barron LD. Molecular light scattering and optical activity. Cambridge, England: Cambridge University Press; 2004. 443 p.
- Berova N, Nakanishi K, Woody RW (editors). Circular dichroism, 2nd ed. New York: Wiley-VCH; 2000. 877 p.
- Polavarapu PL. Optical rotation: recent advances in determining the absolute configuration. *Chirality* 2002;14(10):768–781.
- Lakhtakia A (editor). Selected papers on natural optical activity. SPIE Milestone series 15. Bellingham, WA: SPIE Optical Engineering Press; 1990. 600 p.
- Buckingham AD, Dunn MB. Optical activity of oriented molecules. *J Chem Soc A: Inorg Phys Theor* 1971(12):1988–1991.
- Condon EU. Theories of optical rotatory power. *Rev Mod Phys* 1937;9:432–457.
- Buckingham AD. In: Hirschfelder JO, editor. Advances in chemical physics. Vol 12. New York: Interscience; 1967. p 107–142.
- Rosenfeld L. Theory of electrons. New York: Dover; 1965. 119 p.
- Pershan PS. Nonlinear optical properties of solids: energy considerations. *Phys Rev* 1963;130:919–929.
- Dick B. Irreducible tensor analysis of sum-frequency and difference-frequency-generation in partially oriented samples. *Chem Phys* 1985;96(2):199–215.
- Fischer P. Nonlinear optical properties of chiral media. Ph.D. thesis. Cambridge, England: Cambridge University; 1999.
- Byers JD, Yee HI, Hicks JM. A second-harmonic generation analog of optical-rotatory dispersion for the study of chiral monolayers. *J Chem Phys* 1994;101(7):6233–6241.
- Petralli-Mallow TP, Wong TM, Byers JD, Yee HI, Hicks JM. Circular dichroism spectroscopy at interfaces: a surface second harmonic generation study. *J Phys Chem* 1993;97:1383–1388.
- Giordmaine JA. Nonlinear optical properties of liquids. *Phys Rev* 1965;138(6A):1599–1606.
- Fischer P, Wiersma DS, Righini R, Champagne B, Buckingham AD. Three-wave mixing in chiral liquids. *Phys Rev Lett* 2000;85(20):4253–4256.
- Belkin MA, Kulakov TA, Ernst KH, Yan L, Shen YR. Sum-frequency vibrational spectroscopy on chiral liquids: a novel technique to probe molecular chirality. *Phys Rev Lett* 2000;85(21):4474–4477.
- Belkin MA, Han SH, Wei X, Shen YR. Sum-frequency generation in chiral liquids near electronic resonance. *Phys Rev Lett* 2001; 87:113001.
- Fischer P, Beckwitt K, Wise FW, Albrecht AC. The chiral specificity of sum-frequency generation in solutions. *Chem Phys Lett* 2002; 352(5–6):463–468.
- Fischer P, Wise FW, Albrecht AC. Chiral and achiral contributions to sum-frequency generation from optically active solutions of binaphthol. *J Phys Chem A* 2003;107(40):8232–8238.

27. Belkin MA, Shen YR. Doubly resonant IR-UV sum-frequency vibrational spectroscopy on molecular chirality. *Phys Rev Lett* 2003;91:213907.
28. Fischer P, Buckingham AD, Beckwith K, Wiersma DS, Wise FW. New electro-optic effect: sum-frequency generation from optically active liquids in the presence of a dc electric field. *Phys Rev Lett* 2003;91:173901.
29. Yang PK, Huang JY. Sum-frequency generation from an isotropic chiral medium. *J Opt Soc Am B: Opt Phys* 1998;15(6):1698–1706.
30. Fischer P, Buckingham AD, Albrecht AC. Isotropic second-order nonlinear optical susceptibilities. *Phys Rev A* 2001;64:053816-1–053816-7.
31. Harris RA. Chiral fluctuations in achiral systems. *J Chem Phys* 2001;115(23):10577–10580.
32. Champagne B, Fischer P, Buckingham AD. Ab initio investigation of the sum-frequency hyperpolarizability of small chiral molecules. *Chem Phys Lett* 2000;331(1):83–88.
33. Quinet O, Champagne B. Sum-frequency generation first hyperpolarizability from time-dependent Hartree–Fock method. *Int J Quant Chem* 2001;85(4–5):463–468.
34. Botek E, Champagne B, Turki M, Andre JM. Theoretical study of the second-order nonlinear optical properties of [N]helicenes and [N]phenylenes. *J Chem Phys* 2004;120(4):2042–2048.
35. Byers JD, Hicks JM. Electronic spectral effects on chiral surface second harmonic generation. *Chem Phys Lett* 1994;231:216–224.
36. Hayashi M, Lin SH, Shen YR. Applications of molecular theory of sum-frequency generations to study molecular chirality. *J Phys Chem A* 2004;108(39):8058–8076.
37. Hache F, Mesnil H, Schanne-Klein M-C. Application of classical models of chirality to surface second harmonic generation. *J Chem Phys* 2001;115:6707–6715.
38. Zheng YD, Li JQ, Li CF. Influence of microscopic parameters of chiral molecules with two couple-oscillators model on sum-frequency generation. *Acta Phys Sinica* 2002;51(6):1279–1285.
39. Belkin MA, Shen YR, Flytzanis C. Coupled-oscillator model for nonlinear optical activity. *Chem Phys Lett* 2002;363:479–485.
40. Champagne B, Andre JM, Botek E, Licandro E, Maiorana S, Bossi A, Clays K, Persoons A. Theoretical design of substituted tetrathia-[7]-helicenes with large second-order nonlinear optical responses. *ChemPhysChem* 2004;5(9):1438–1442.
41. Buckingham AD, Fischer P. Linear electro-optic effect in optically active liquids. *Chem Phys Lett* 1998;297(3–4):239–246.
42. Belkin MA, Kulakov TA, Ernst KH, Han SH, Shen YR. Resonant sum-frequency generation in chiral liquids. *Opt Mater* 2003;21(1–3):1–5.
43. Belkin MA, Shen YR, Harris RA. Sum-frequency vibrational spectroscopy of chiral liquids off and close to electronic resonance and the antisymmetric Raman tensor. *J Chem Phys* 2004;120(21):10118–10126.
44. Cho MH. Time-resolved vibrational optical activity measurement by the infrared-visible sum-frequency-generation with circularly polarized infrared light. *J Chem Physics* 2002;116(4):1562–1570.
45. Shen YR. Surfaces probed by nonlinear optics. *Surf Sci* 1994;299/300:551–562.
46. Heinz TF. Second-order nonlinear optical effects at surfaces and interfaces. In: Ponath HE, Stegeman GI, editors. *Nonlinear surface electromagnetic phenomena*. Amsterdam, The Netherlands: North Holland; 1991. p 353–416.
47. Byers JD, Yee HI, Hicks JM. A second harmonic generation analog of optical rotatory dispersion for the study of chiral monolayers. *J Chem Phys* 1994;101:6233–6241.
48. Kauranen M, Van Elshocht S, Maki JJ, Persoons A. Second-harmonic generation from chiral surfaces. *J Chem Phys* 1994;101:8193–8199.
49. Hecht L, Barron LD. New aspects of second harmonic optical activity from chiral surfaces and interfaces. *Mol Phys* 1996;89:61–80.
50. Byers JD, Yee HI, Petralli-Mallow T, Hicks JM. Second-harmonic generation circular-dichroism spectroscopy from chiral monolayers. *Phys Rev B* 1994;49(20):14643–14647.
51. Svirko YP, Zheludev NI. *Polarization of light in nonlinear optics*. Chichester, England: Wiley; 1998. 240 p.
52. Schanne-Klein MC, Mesnil H, Boulesteix T, Hache F. Nonlinear optical spectroscopy of chiral molecules. *Recent Res Dev Chem Phys* 2003;4:487–517.
53. Kriech MA, Conboy JC. Counterpropagating second-harmonic generation: a new technique for the investigation of molecular chirality at surfaces. *J Opt Soc Am B* 2004;21:1013–1022.
54. Kauranen M, Maki JJ, Verbiest T, Van Elshocht S, Persoons A. Quantitative determination of electric and magnetic second-order susceptibility tensors of chiral surfaces. *Phys Rev B* 1997;55:R1985–1988.
55. Schanne-Klein MC, Hache F, Roy A, Flytzanis C, Payrastré C. Off resonance second order optical activity of isotropic layers of chiral molecules: observation of electric and magnetic contributions. *J Chem Phys* 1998;108(22):9436–9443.
56. Van Elshocht S, Verbiest T, Kauranen M, Persoons A. Direct evidence of the failure of electric-dipole approximation in second harmonic generation from a chiral polymer film. *J Chem Phys* 1997;107:8201–8203.
57. Eliel EL, Wilen SH. *Stereochemistry of organic compounds*. New York: Wiley; 1994. 1020 p.
58. Hache F, Boulesteix T, Schanne-Klein MC, Alexandre M, Lemerrier G, Andraud C. Polarization rotation in a second harmonic reflection experiment from an isotropic surface of chiral Tröger base. *J Phys Chem B* 2003;107(22):5261–5266.
59. Schanne-Klein MC, Hache F, Brotin T, Andraud C, Collet A. Magnetic chiroptical effects in surface second harmonic reflection. *Chem Phys Lett* 2001;338(2–3):159–166.
60. Van Elshocht S, Kauranen M, Van Rompaey Y, Persoons A. Optical activity of anisotropic achiral surfaces. *Phys Rev Lett* 1996;77:1456–1459.
61. Verbiest T, Kauranen M, Persoons A. Optical activity of anisotropic achiral surfaces. *J Opt Soc Am B* 1998;15:451–457.
62. Fischer P, Buckingham AD. Surface second-order nonlinear activity. *J Opt Soc Am B* 1998;15:2951–2957.
63. Simpson GJ. Structural origin of circular dichroism in surface second harmonic generation. *J Chem Phys* 2002;117:3398–3410.
64. Kauranen M, Van Elshocht S, Verbiest T, Persoons A. Tensor analysis of the second order nonlinear optical susceptibility of chiral anisotropic films. *J Chem Phys* 2000;112:1497–1502.
65. Siltanen M, Cattaneo S, Vuorimaa E, Lemmetyinen H, Katz TJ, Phillips KES, Kauranen M. A regression technique to analyze the second-order nonlinear optical response of thin films. *J Chem Phys* 2004;121:1–4.
66. Simpson GJ. Molecular origins of the remarkable chiral sensitivity of second-order nonlinear optics. *ChemPhysChem* 2004;5(9):1301–1310.
67. Han SH, Ji N, Belkin MA, Shen YR. Sum-frequency spectroscopy of electronic resonances on a chiral surface monolayer of bi-naphthol. *Phys Rev B* 2002;66:165415-1–165415-6.
68. Busson B, Kauranen M, Nuckolls C, Katz TJ, Persoons A. Quasi-phase-matching in chiral materials. *Phys Rev Lett* 2000;84:79–82.
69. Ostroverkhov V, Petschek RG, Singer KD, Twieg RJ. Lambda-like chromophores for chiral non-linear optical materials. *Chem Phys Lett* 2001;340:109–115.
70. Koetzelberghs G, Sioncke S, Verbiest T, Persoons A, Samyn C. Synthesis and properties of chiral helical chromophore-functionalised polybinaphthalenes for second-order nonlinear optical applications. *Polymer* 2003;44:3785–3794.
71. Crawford MJ, Haslam S, Probert JM, Gruzdkov YA, Frey JG. Second harmonic generation from the air/water interface of an aqueous solution of the dipeptide Boc-Trp-Trp. *Chem Phys Lett* 1994;230:260–264.
72. Petralli-Mallow TP, Plant AL, Lewis ML, Hicks JM. Cytochrome c at model membrane surfaces: exploration via second harmonic generation-circular dichroism and surface-enhanced resonance Raman spectroscopy. *Langmuir* 2000;16:5960–5966.

73. Polizzi MA, Plochinik RM, Simpson GJ. Ellipsometric approach for the real-time detection of label-free protein adsorption by second harmonic generation. *J Am Chem Soc* 2004;126:5001–5007.
74. Kriech MA, Conboy JC. Imaging chirality with second-harmonic generation microscopy. *J Am Chem Soc* 2005;125:2834–2835.
75. Akhmanov SA, Zharikov VI. Nonlinear optics in gyrotropic media. *JETP Lett* 1967;6:137–140.
76. Atkins PW, Barron LD. Quantum field theory of optical birefringence phenomena. I. Linear and nonlinear optical rotation. *Proc R Soc A* 1968;304:303–317.
77. Wagniere G. Optical activity of higher-order in a medium of randomly oriented molecules. *J Chem Phys* 1982;77(6):2786–2792.
78. Akhmanov SA, Lyakhov GA, Makarov VA, Zharikov VI. Theory of nonlinear optical activity in isotropic media and liquid crystals. *Opt Acta* 1982;29:1359–1369.
79. Vlasov DV, Zaitsev VP. Experimental observation of nonlinear optical activity. *JETP Lett* 1971;14:112–115.
80. Cameron R, Tabisz GC. Observation of two-photon optical rotation by molecules. *Mol Phys* 1996;90:159–164.
81. Mesnil H, Hache F. Experimental evidence of third-order nonlinear circular dichroism in a liquid of chiral molecules. *Phys Rev Lett* 2000;85:4257–4260.
82. Hache F, Mesnil H, Schanne-Klein M-C. Nonlinear circular dichroism in a liquid of chiral molecules: a theoretical investigation. *Phys Rev B* 1999;60:6405–6411.
83. Mesnil H, Schanne-Klein MC, Hache F, Alexandre M, Lemerrier G, Andraud C. Experimental observation of nonlinear circular dichroism in a pump–probe experiment. *Chem Phys Lett* 2001;338(4–6):269–276.
84. Markowicz PP, Samoc M, Cerne J, Prasad PN, Pucci A, Ruggeri G. Modified Z-scan techniques for investigations of nonlinear chiroptical effects. *Opt Express* 2004;12(21):5209–5214.
85. Cho M. Two-dimensional circularly polarized pump–probe spectroscopy. *J Chem Phys* 2003;119:7003–7016.
86. Meijer EW, Feringa BL. Chirality in nonlinear optics and optical switching. *Mol Cryst Liq Cryst* 1993;235:169–180.
87. Tran P. All-optical switching with a nonlinear chiral photonic bandgap structure. *J Opt Soc Am B* 1999;16:70–73.
88. Lewis JW, Golbeck RA, Kliger DS, Xie X, Dunn RC, Simon JD. Time-resolved circular dichroism spectroscopy: experiment, theory and applications to biological systems. *J Phys Chem* 1992;96:5243–5254.
89. Milder SJ, Bjorling SC, Kuntz ID, Kliger DS. Time-resolved circular dichroism and absorption studies of the photolysis reaction of (carbonmonoxy) myoglobin. *Biophys J* 1988;53:659–664.
90. Xie X, Simon JD. Picosecond time-resolved circular dichroism study of protein relaxation in myoglobin following photodissociation of CO. *J Am Chem Soc* 1990;112:7802–7803.
91. Hache F, Dartigalongue T. Application of the polarizability theory to the calculation of anisotropic circular dichroism spectra. *Chem Phys* 2004;303(1–3):197–203.
92. Applequist J, Sundberg KR, Olson ML, Weiss LC. A normal mode treatment of optical properties of a classical coupled oscillator system with Lorentzian bandshapes. *J Chem Phys* 1979;70:1240–1246.
93. Bjarnason JO, Andersen HC, Hudson BS. Quantum theory of coherent Raman scattering by optically active isotropic materials. *J Chem Phys* 1980;72(7):4132–4140.
94. Oudar JL, Minot C, Garetz BA. Polarization spectroscopy as a probe of Raman optical activity. *J Chem Phys* 1982;76(5):2227–2237.
95. Barron LD, Hecht L. Vibrational Raman optical activity: from fundamentals to biochemical applications. In: Berova N, Nakanishi K, Woody RW, editors. *Circular dichroism*. 2nd ed. New York: Wiley-VCH; 2000. p 877.
96. Nafie LA. Infrared and Raman vibrational optical activity: theoretical and experimental aspects. *Annu Rev Phys Chem* 1997;48:357–386.
97. Levenson MD. *Introduction to nonlinear laser spectroscopy*. New York: Academic Press; 1982. 256 p.
98. Spiegel H, Schneider FW. First measurement of Raman optical activity by CARS. In: Bertoluzza A, Fagnano C, Monti P, editors. *Spectroscopy of biological molecules—state of the art*. New York: John Wiley and Sons; 1989. p 317–322.
99. Koroteev NI. Novel nonlinear optical techniques for studying chiral molecules of biological importance. In: Walther H, Koroteev NI, Scully M, editors. *Frontiers in nonlinear optics*. The Sergei Akhmanov memorial volume. Bristol, England: Institute of Physics Publishing; 1993. p 228–239.
100. Romero LCD, Meech SR, Andrews DL. Five-wave mixing in molecular fluids. *J Phys B: Atom Mol Opt Phys* 1997;30(23):5609–5619.
101. Shkurinov AP, Dubrovskii AV, Koroteev NI. Second harmonic generation in an optically active liquid: experimental observation of a 4th-order optical nonlinearity due to molecular chirality. *Phys Rev Lett* 1993;70(8):1085–1088.
102. Rentzepis PM, Giordmaine JA, Wecht KW. Coherent optical mixing in optically active liquids. *Phys Rev Lett* 1966;16(18):792–794.
103. Koroteev NI. BioCARS—a novel nonlinear optical technique to study vibrational spectra of chiral biological molecules in solution. *Biospectroscopy* 1995;1(5):341–350.
104. Volkov SN, Konovalov NI, Koroteev NI, Makarov VA. Model calculation of the optical susceptibilities taking account of the spatial dispersion of nonlinearity in nonlinear spectroscopy of solutions of chiral molecules. *Quantum Electron* 1995;25:62–65.
105. Zheltikov AM, Naumov AN. Waveguide solution of the Koroteev problem in the nonlinear optics of media with broken mirror symmetry: collinear three- and five-wave mixing schemes in planar waveguides. *Quantum Electron* 1999;29:607–612.
106. Wang J, Chen XY, Clarke ML, Chen Z. Detection of chiral sum frequency generation vibrational spectra of proteins and peptides at interfaces in situ. *Proc Nat Acad Sci* 2005;102:4978–4983.
107. Mitchell SA, McAloney RA, Moffatt D, Mora-Diez N, Zgierski MZ. Second-harmonic generation optical activity of a polypeptide α -helix at the air/water interface. *J Chem Phys* 2005;122:114707.
108. Abramavicius D, Mukamel S. Coherent third-order spectroscopic probes of molecular chirality. *J Chem Phys* 2005;122:134305.
109. Simpson GJ, Perry JM, Moad AJ, Wampler RD. Uncoupled oscillator model for interpreting second harmonic generation measurements of oriented chiral systems. *Chem Phys Lett* 2004;399:26–32.